

moment has to be attributed solely to spin-crossover origins. Then some support is given to the model used in fitting the μ vs T data and based on a Boltzmann distribution over two states, each characterized by a constant moment.

Finally, there is no doubt that, in spite of some weak differences between powdered sample and solution, the magnetic properties of $[(AE)_2Fe]^+$ must be described in terms of high-spin ($S = 5/2$) to low-spin ($S = 1/2$) conversion, in both cases. The studies of

the anomalies observed for ground crystals will be the subject of a future examination.

Registry No. $[(AE)_2Fe]BPh_4$, 127182-79-0.

Supplementary Material Available: Tables of atomic coordinates, thermal parameters, bond lengths and angles, and least-squares planes (5 pages); a structure factor table (19 pages). Ordering information is given on any current masthead page.

Contribution from the Department of Chemistry, Columbia University, New York, New York 10027

(Tris(3-*tert*-butylpyrazolyl)hydroborato)manganese(II), -iron(II), -cobalt(II), and -nickel(II) Halide Derivatives: Facile Abstraction of Fluoride from $[BF_4]^-$

Ian B. Gorrell and Gerard Parkin*

Received November 7, 1989

The complexes $\{\eta^3\text{-HB}(3\text{-Bu}^t\text{pz})_3\}MCl$ ($M = Mn, Fe, Co, Ni$) have been prepared by metathesis of MCl_2 with $Tl\{\text{HB}(3\text{-Bu}^t\text{pz})_3\}$. Reaction of $\{\eta^3\text{-HB}(3\text{-Bu}^t\text{pz})_3\}MCl$ ($M = Fe, Co$) with $AgBF_4$ results in fluoride abstraction and the formation of $\{\eta^3\text{-HB}(3\text{-Bu}^t\text{pz})_3\}MF$. The molecular structures of the complexes $\{\eta^3\text{-HB}(3\text{-Bu}^t\text{pz})_3\}FeCl$, $\{\eta^3\text{-HB}(3\text{-Bu}^t\text{pz})_3\}CoCl$, and $\{\eta^3\text{-HB}(3\text{-Bu}^t\text{pz})_3\}CoF$ have been determined by single-crystal X-ray diffraction studies. Crystal data for $\{\eta^3\text{-HB}(3\text{-Bu}^t\text{pz})_3\}FeCl$: $C_{21}H_{34}N_6BF_2Cl$; $a = 16.075$ (5), $b = 15.958$ (4), $c = 9.792$ (4) Å; orthorhombic, space group $Pnma$ (No. 62); $Z = 4$. Crystal data for $\{\eta^3\text{-HB}(3\text{-Bu}^t\text{pz})_3\}CoCl$: $C_{21}H_{34}N_6BCoCl$; $a = 16.024$ (1), $b = 15.966$ (3), $c = 9.769$ (4) Å; orthorhombic, space group $Pnma$ (No. 62); $Z = 4$. Crystal data for $\{\eta^3\text{-HB}(3\text{-Bu}^t\text{pz})_3\}CoF$: $C_{21}H_{34}N_6BCoF$; $a = 18.402$ (5), $b = 15.414$ (6), $c = 9.722$ (1) Å; $\beta = 100.24$ (3)°; monoclinic, space group $P1n1$ (No. 7); $Z = 2$.

Introduction

The coordination chemistry of poly(pyrazolyl)hydroborato ligands with the transition metals has developed extensively since their introduction by Trofimenko.¹ In particular, the tris(pyrazolyl)hydroborato ligand is often considered as a cyclopentadienyl analogue in that both ligands effectively occupy three coordination sites around a metal center and are both 5-electron donors.² Alkyl-substituted derivatives of the cyclopentadienyl ligand, and most notably the pentamethylcyclopentadienyl ligand, have been successfully utilized to allow the formation of monomeric transition-metal complexes that may not be accessible for the unsubstituted cyclopentadienyl derivatives. The cone angles of the alkyl-substituted η^3 -tris(pyrazolyl)hydroborato ligands $\eta^3\text{-HB}(\text{pz})_3$, $\eta^3\text{-HB}(3,5\text{-Me}_2\text{pz})_3$, and $\eta^3\text{-HB}(3\text{-Bu}^t\text{pz})_3$ have been estimated as 184, 224, and 244°, respectively, and are significantly larger than the cone angles of 100 and 142° for the $\eta^5\text{-C}_5\text{H}_5$ and $\eta^5\text{-C}_5\text{Me}_5$ ligands.^{3,4} It is, therefore, to be expected that the greater steric demands of the η^3 -tris(pyrazolyl)hydroborato ligands may allow the isolation of unusual derivatives that are not accessible for the cyclopentadienyl counterparts. For example, Curtis et al. have demonstrated that the $\eta^3\text{-HB}(3,5\text{-Me}_2\text{pz})_3$ ligand is capable of stabilizing a 17-electron radical, $\{\eta^3\text{-HB}(3,5\text{-Me}_2\text{pz})_3\}Mo(CO)_3$.⁵ Here we report the use of the tris(3-*tert*-butylpyrazolyl)hydroborato ligand in the preparation of half-sandwich halide derivatives of manganese, iron, cobalt, and nickel, $\{\eta^3\text{-HB}(3\text{-Bu}^t\text{pz})_3\}MCl$ ($M = Mn, Fe, Co, Ni$).

Results and Discussion

Several (poly(pyrazolyl)hydroborato)iron complexes have been reported, of which the 6-coordinate, 18-electron derivatives

Table I. Atom Coordinates ($\times 10^4$) and Temperature Factors ($\text{Å}^2 \times 10^3$) for $\{\eta^3\text{-HB}(3\text{-Bu}^t\text{pz})_3\}FeCl$

atom	<i>x</i>	<i>y</i>	<i>z</i>	<i>U</i> ^a
Fe	1588 (1)	7500	5931 (1)	41 (1)
Cl	256 (1)	7500	5306 (2)	85 (1)
N(11)	3303 (4)	7500	5120 (6)	47 (3)
N(12)	2540 (4)	7500	4490 (6)	47 (2)
N(21)	2981 (3)	8288 (3)	7265 (4)	45 (2)
N(22)	2147 (3)	8446 (3)	4088 (4)	41 (2)
C(11)	3908 (5)	7500	4194 (10)	57 (3)
C(12)	3553 (6)	7500	2924 (10)	64 (4)
C(13)	2700 (5)	7500	3140 (7)	51 (3)
C(14)	1999 (6)	7500	2113 (7)	63 (4)
C(15)	2356 (6)	7500	655 (8)	104 (5)
C(16)	1468 (4)	6718 (4)	2292 (6)	89 (3)
C(21)	3310 (4)	8882 (4)	8060 (5)	58 (2)
C(22)	2705 (4)	9438 (4)	8394 (6)	59 (2)
C(23)	1980 (3)	9152 (4)	7782 (5)	45 (2)
C(24)	1114 (4)	9534 (4)	7865 (5)	53 (2)
C(25)	512 (3)	8889 (4)	8435 (5)	61 (2)
C(26)	1133 (4)	10289 (4)	8851 (7)	100 (3)
C(27)	843 (4)	9826 (4)	6464 (6)	102 (3)
B	3391 (6)	7500	6668 (9)	46 (3)

^aEquivalent isotropic *U* defined as one-third of the trace of the orthogonalized U_{ij} tensor.

Table II. Bond Lengths (Å) for $\{\eta^3\text{-HB}(3\text{-Bu}^t\text{pz})_3\}FeCl$

Fe-Cl	2.227 (2)	Fe-N(12)	2.083 (6)
Fe-N(22)	2.091 (4)	Fe-N(22')	2.091 (4)
N(11)-N(12)	1.373 (9)	N(11)-C(11)	1.329 (11)
N(11)-B	1.522 (11)	N(12)-C(13)	1.347 (9)
N(21)-N(22)	1.375 (6)	N(21)-C(21)	1.335 (7)
N(21)-B	1.535 (7)	N(22)-C(23)	1.343 (7)
C(11)-C(12)	1.368 (13)	C(12)-C(13)	1.388 (13)
C(13)-C(14)	1.509 (12)	C(14)-C(15)	1.538 (11)
C(14)-C(16)	1.523 (9)	C(14)-C(16')	1.523 (9)
C(21)-C(22)	1.356 (9)	C(22)-C(23)	1.388 (8)
C(23)-C(24)	1.521 (8)	C(24)-C(25)	1.519 (8)
C(24)-C(26)	1.545 (9)	C(24)-C(27)	1.512 (8)
B-N(21')	1.535 (7)		

$\{\eta^3\text{-HB}(\text{pz})_3\}_2Fe^6$ and $\{\eta^3\text{-HB}(3,5\text{-Me}_2\text{pz})_3\}_2Fe^7$ may be viewed as analogues of ferrocene. The effect of increasing the size of the

- (1) (a) Trofimenko, S. *Acc. Chem. Res.* **1971**, *4*, 17-22. (b) Trofimenko, S. *Chem. Rev.* **1972**, *72*, 497-509. (c) Trofimenko, S. *Prog. Inorg. Chem.* **1986**, *34*, 115-210. (d) Shaver, A. *Comprehensive Coordination Chemistry*; Wilkinson, G., Gillard, R. D.; McCleverty, J. A., Eds.; Pergamon Press: Oxford, England, 1987; Vol. 2, pp 245-259. (e) Shaver, A. *J. Organomet. Chem. Libr.* **1977**, *3*, 157-188.
- (2) Electron counting is according to a neutral ligand formalism.
- (3) Trofimenko, S.; Calabrese, J. C.; Thompson, J. S. *Inorg. Chem.* **1987**, *26*, 1507-1514.
- (4) (a) Frauendorfer, E.; Brunner, H. *J. Organomet. Chem.* **1982**, *240*, 371-379. (b) Davies, C. E.; Gardiner, I. M.; Green, J. C.; Green, M. L. H.; Hazel, N. J.; Grebenik, P. D.; Mtetwa, V. S.; Prout, K. *J. Chem. Soc., Dalton Trans.* **1985**, 669-683.
- (5) Shiu, K.-B.; Curtis, M. D.; Huffman, J. C. *Organometallics* **1983**, *2*, 936-938.

(6) Trofimenko, S. *J. Am. Chem. Soc.* **1967**, *89*, 3148-3158.

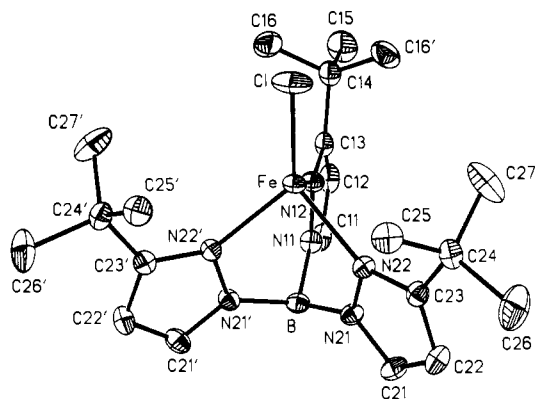


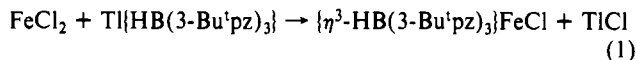
Figure 1. ORTEP diagram of $\{\eta^3\text{-HB}(3\text{-Bu}^t\text{pz})_3\}\text{FeCl}$. For clarity, thermal ellipsoids are shown at 20% probability.

Table III. Bond Angles (deg) for $\{\eta^3\text{-HB}(3\text{-Bu}^t\text{pz})_3\}\text{FeCl}$

Cl-Fe-N(12)	121.4 (2)	Cl-Fe-N(22)	124.2 (1)
N(12)-Fe-N(22)	92.9 (2)	Cl-Fe-N(22')	124.2 (1)
N(12)-Fe-N(22')	92.9 (2)	N(22)-Fe-N(22')	92.4 (2)
N(12)-N(11)-C(11)	110.3 (6)	N(12)-N(11)-B	122.0 (6)
C(11)-N(11)-B	127.7 (7)	Fe-N(12)-N(11)	110.7 (4)
Fe-N(12)-C(13)	143.6 (6)	N(11)-N(12)-C(13)	105.7 (6)
N(22)-N(21)-C(21)	109.2 (4)	N(22)-N(21)-B	121.4 (5)
C(21)-N(21)-B	129.3 (5)	Fe-N(22)-N(21)	110.8 (3)
Fe-N(22)-C(23)	142.5 (4)	N(21)-N(22)-C(23)	106.6 (4)
N(11)-C(11)-C(12)	108.3 (7)	C(11)-C(12)-C(13)	105.9 (8)
N(12)-C(13)-C(12)	109.7 (7)	N(12)-C(13)-C(14)	120.8 (7)
C(12)-C(13)-C(14)	129.5 (7)	C(13)-C(14)-C(15)	109.9 (8)
C(13)-C(14)-C(16)	110.0 (4)	C(15)-C(14)-C(16)	108.4 (4)
C(13)-C(14)-C(16')	110.0 (4)	C(15)-C(14)-C(16')	108.4 (4)
C(16)-C(14)-C(16')	110.1 (8)	N(21)-C(21)-C(22)	108.8 (5)
C(21)-C(22)-C(23)	106.4 (5)	N(22)-C(23)-C(22)	109.0 (5)
N(22)-C(23)-C(24)	123.1 (5)	C(22)-C(23)-C(24)	127.9 (5)
C(23)-C(24)-C(25)	109.3 (5)	C(23)-C(24)-C(26)	109.1 (5)
C(25)-C(24)-C(26)	108.2 (5)	C(23)-C(24)-C(27)	109.8 (4)
C(25)-C(24)-C(27)	111.0 (5)	C(26)-C(24)-C(27)	109.4 (5)
N(11)-B-N(21)	109.9 (5)	N(11)-B-N(21')	109.9 (5)
N(21)-B-N(21')	110.0 (7)		

alkyl substituent of the pyrazolyl group is dramatically illustrated by the fact that $\{\eta^3\text{-HB}(\text{pz})_3\}_2\text{Fe}$ is magenta and exhibits "spin equilibrium" between high- and low-spin forms, whereas $\{\eta^3\text{-HB}(3,5\text{-Me}_2\text{pz})_3\}_2\text{Fe}$ is colorless, with a high-spin ground state. In contrast to the above sandwich complexes, the half-sandwich derivatives $\{\eta^3\text{-HB}(\text{pz})_3\}\text{FeX}$ and $\{\eta^3\text{-HB}(3,5\text{-Me}_2\text{pz})_3\}\text{FeX}$ (X = halogen) are unknown. Thus, we were particularly interested in utilizing the steric demands of the η^3 -tris(3-*tert*-butylpyrazolyl)hydroborato ligand to allow the synthesis of the half-sandwich derivative $\{\eta^3\text{-HB}(3\text{-Bu}^t\text{pz})_3\}\text{FeCl}$.

The complex $\{\eta^3\text{-HB}(3\text{-Bu}^t\text{pz})_3\}\text{FeCl}$ is readily obtained by the reaction of FeCl_2 with $\text{Ti}\{\text{HB}(3\text{-Bu}^t\text{pz})_3\}$ in acetone (eq 1). The



molecular structure of $\{\eta^3\text{-HB}(3\text{-Bu}^t\text{pz})_3\}\text{FeCl}$ has been determined by single-crystal X-ray diffraction (Figure 1) and confirms both the monomeric nature of the complex and the η^3 -coordination mode of the tris(pyrazolyl)hydroborato ligand. Atomic coordinates and thermal parameters for non-hydrogen atoms are listed in Table I, and selected bond distances and angles are listed in Tables II and III. The iron center is trigonally distorted tetrahedral, as evidenced by the N-Fe-Cl (121.4–124.2°) and N-Fe-N bond angles (92.4–92.9°).

In terms of the tris(pyrazolyl)hydroborato/cyclopentadienyl analogy, $\{\eta^3\text{-HB}(3\text{-Bu}^t\text{pz})_3\}\text{FeCl}$ represents a 14-electron iron complex, which has no parallel in (η^5 -cyclopentadienyl)iron chemistry, and may thus provide an entry to 14-electron iron alkyl

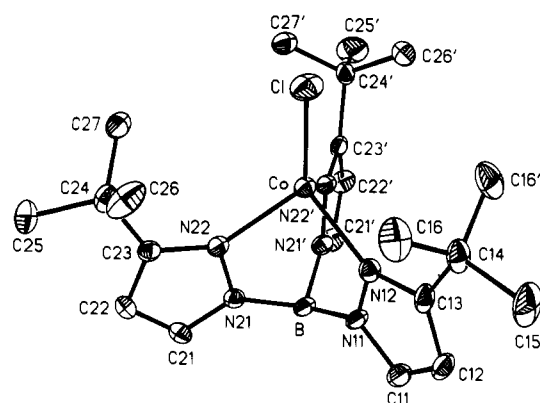


Figure 2. ORTEP diagram of $\{\eta^3\text{-HB}(3\text{-Bu}^t\text{pz})_3\}\text{CoCl}$. For clarity, thermal ellipsoids are shown at 20% probability.

Table IV. Atom Coordinates ($\times 10^4$) and Temperature Factors ($\text{\AA}^2 \times 10^3$) for $\{\eta^3\text{-HB}(3\text{-Bu}^t\text{pz})_3\}\text{CoCl}$

atom	x	y	z	U^a
Co	3362 (1)	2500	962 (1)	39 (1)
Cl	4696 (1)	2500	368 (2)	74 (1)
N(11)	1685 (3)	2500	134 (6)	47 (2)
N(12)	2460 (4)	2500	-493 (6)	45 (2)
N(21)	2011 (2)	1711 (3)	2286 (4)	43 (1)
N(22)	2845 (2)	1558 (2)	2097 (3)	41 (1)
C(11)	1082 (5)	2500	-826 (9)	59 (3)
C(12)	1456 (5)	2500	-2081 (8)	62 (3)
C(13)	2317 (5)	2500	-1863 (7)	53 (3)
C(14)	3019 (5)	2500	-2881 (7)	61 (3)
C(15)	2667 (6)	2500	-4338 (7)	98 (5)
C(16)	3561 (4)	1714 (4)	-2684 (5)	86 (3)
C(21)	1686 (3)	1118 (3)	3062 (5)	54 (2)
C(22)	2285 (3)	559 (4)	3398 (5)	58 (2)
C(23)	3019 (3)	849 (3)	2785 (5)	45 (2)
C(24)	3883 (3)	467 (3)	2862 (5)	52 (2)
C(25)	3857 (4)	-282 (4)	3828 (7)	97 (3)
C(26)	4165 (4)	197 (4)	1458 (6)	93 (3)
C(27)	4490 (3)	1108 (3)	3447 (5)	59 (2)
B	1589 (5)	2500	1699 (9)	45 (3)

^a Equivalent isotropic U defined as one-third of the trace of the orthogonalized U_{ij} tensor.

Table V. Bond Lengths (\AA) for $\{\eta^3\text{-HB}(3\text{-Bu}^t\text{pz})_3\}\text{CoCl}$

Co-Cl	2.216 (2)	Co-N(12)	2.028 (6)
Co-N(22)	2.043 (4)	Co-N(22')	2.043 (4)
N(11)-N(12)	1.385 (8)	N(11)-C(11)	1.346 (10)
N(11)-B	1.536 (10)	N(12)-C(13)	1.357 (9)
N(21)-N(22)	1.371 (5)	N(21)-C(21)	1.320 (6)
N(21)-B	1.540 (6)	N(22)-C(23)	1.347 (6)
C(11)-C(12)	1.364 (12)	C(12)-C(13)	1.396 (12)
C(13)-C(14)	1.502 (11)	C(14)-C(15)	1.531 (10)
C(14)-C(16)	1.539 (8)	C(14)-C(16')	1.539 (8)
C(21)-C(22)	1.351 (7)	C(22)-C(23)	1.398 (7)
C(23)-C(24)	1.516 (7)	C(24)-C(25)	1.524 (8)
C(24)-C(26)	1.507 (7)	C(24)-C(27)	1.523 (7)
B-N(21')	1.540 (6)		

derivatives $\{\eta^3\text{-HB}(3\text{-Bu}^t\text{pz})_3\}\text{FeR}$.

The manganese derivative, $\{\eta^3\text{-HB}(3\text{-Bu}^t\text{pz})_3\}\text{MnCl}$, and the previously reported cobalt and nickel derivatives, $\{\eta^3\text{-HB}(3\text{-Bu}^t\text{pz})_3\}\text{CoCl}$ and $\{\eta^3\text{-HB}(3\text{-Bu}^t\text{pz})_3\}\text{NiCl}$,³ have also been synthesized by a similar procedure, and the cobalt derivative has been characterized by X-ray diffraction (Figure 2). Atomic coordinates and thermal parameters for non-hydrogen atoms are listed in Tables IV, and selected bond distances and angles are listed in Tables V and VI. The structure of $\{\eta^3\text{-HB}(3\text{-Bu}^t\text{pz})_3\}\text{CoCl}$ is similar to those of $\{\eta^3\text{-HB}(3\text{-Bu}^t\text{pz})_3\}\text{FeCl}$ and the previously reported cobalt derivative, $\{\eta^3\text{-HB}(3\text{-Bu}^t\text{pz})_3\}\text{Co}(\text{NCS})$.³

The iron and cobalt complexes $\{\eta^3\text{-HB}(3\text{-Bu}^t\text{pz})_3\}\text{MCl}$ (M = Fe, Co) undergo a rapid chloride-abstraction reaction with AgBF_4 . However, the products are not the 3-coordinate cations, $[\{\eta^3\text{-}$

(7) Trofimenko, S. *J. Am. Chem. Soc.* **1967**, *89*, 6288–6294.

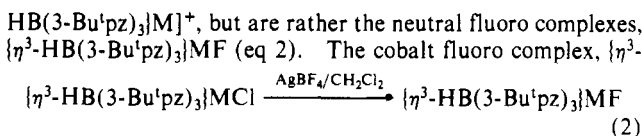
Table VI. Bond Angles (deg) for $\{\eta^3\text{-HB(3-Bu}^i\text{pz)}_3\}\text{CoCl}$

Cl-Co-N(12)	120.3 (2)	Cl-Co-N(22)	122.2 (1)
N(12)-Co-N(22)	95.3 (1)	Cl-Co-N(22')	122.2 (1)
N(12)-Co-N(22')	95.3 (1)	N(22)-Co-N(22')	94.8 (2)
N(12)-N(11)-C(11)	109.5 (6)	N(12)-N(11)-B	122.0 (6)
C(11)-N(11)-B	128.5 (6)	Co-N(12)-N(11)	109.2 (4)
Co-N(12)-C(13)	144.3 (5)	N(11)-N(12)-C(13)	106.6 (6)
N(22)-N(21)-C(21)	109.6 (4)	N(22)-N(21)-B	121.5 (4)
C(21)-N(21)-B	128.8 (5)	Co-N(22)-N(21)	109.7 (3)
Co-N(22)-C(23)	143.8 (3)	N(21)-N(22)-C(23)	106.5 (4)
N(11)-C(11)-C(12)	108.2 (7)	C(11)-C(12)-C(13)	107.2 (7)
N(12)-C(13)-C(12)	108.5 (7)	N(12)-C(13)-C(14)	121.8 (7)
C(12)-C(13)-C(14)	129.7 (7)	C(13)-C(14)-C(15)	109.9 (7)
C(13)-C(14)-C(16)	109.9 (4)	C(15)-C(14)-C(16)	108.9 (4)
C(13)-C(14)-C(16')	109.9 (4)	C(15)-C(14)-C(16')	108.9 (4)
C(16)-C(14)-C(16')	109.3 (7)	N(21)-C(21)-C(22)	109.4 (4)
C(21)-C(22)-C(23)	105.9 (5)	N(22)-C(23)-C(22)	108.6 (4)
N(22)-C(23)-C(24)	123.5 (4)	C(22)-C(23)-C(24)	127.9 (5)
C(23)-C(24)-C(25)	108.8 (4)	C(23)-C(24)-C(26)	110.1 (4)
C(25)-C(24)-C(26)	110.3 (5)	C(23)-C(24)-C(27)	109.3 (4)
C(25)-C(24)-C(27)	108.3 (4)	C(26)-C(24)-C(27)	110.0 (4)
N(11)-B-N(21)	109.1 (4)	N(11)-B-N(21')	109.1 (4)
N(21)-B-N(21')	109.7 (6)		

Table VII. Atom Coordinates ($\times 10^4$) and Temperature Factors ($\text{\AA}^2 \times 10^3$) for $\{\eta^3\text{-HB(3-Bu}^i\text{pz)}_3\}\text{CoF}$

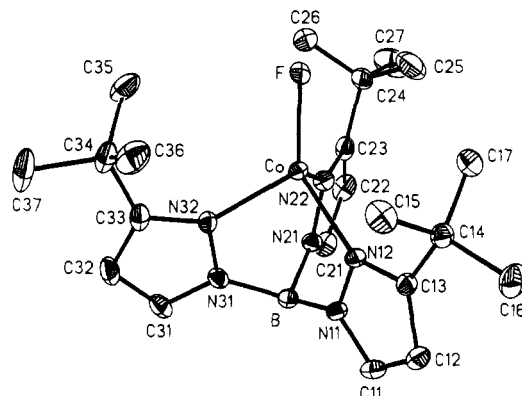
atom	x	y	z	U^a
Co	350	2356 (1)	4954	36 (1)
F	-1905 (3)	2027 (2)	5343 (3)	41 (1)
N(11)	2451 (6)	3493 (3)	3862 (5)	38 (1)
N(12)	792 (5)	3422 (3)	3825 (4)	37 (1)
N(21)	3202 (6)	1913 (3)	3876 (5)	42 (2)
N(22)	1702 (6)	1552 (3)	3955 (5)	41 (2)
N(31)	3578 (6)	2785 (3)	6173 (5)	41 (2)
N(32)	2156 (6)	2619 (3)	6624 (4)	40 (1)
C(11)	2719 (8)	4199 (4)	3125 (6)	47 (2)
C(12)	1256 (8)	4599 (4)	2627 (7)	50 (2)
C(13)	64 (7)	4087 (4)	3071 (5)	39 (2)
C(14)	-1746 (7)	4209 (4)	2850 (6)	45 (2)
C(15)	-2232 (8)	4446 (5)	4253 (7)	62 (3)
C(16)	-2244 (10)	4954 (5)	1801 (8)	78 (3)
C(17)	-2621 (8)	3382 (4)	2262 (7)	56 (2)
C(21)	4108 (8)	1356 (4)	3359 (7)	55 (2)
C(22)	3206 (10)	631 (4)	2944 (7)	64 (3)
C(23)	1689 (9)	770 (4)	3303 (6)	52 (2)
C(24)	168 (9)	198 (4)	3121 (7)	59 (2)
C(25)	-1272 (11)	712 (6)	2424 (11)	101 (4)
C(26)	-44 (12)	-169 (7)	4481 (8)	104 (4)
C(27)	405 (13)	-564 (6)	2113 (12)	131 (6)
C(31)	4757 (8)	2882 (4)	7274 (7)	55 (2)
C(32)	4101 (9)	2799 (4)	8460 (7)	61 (2)
C(33)	2477 (9)	2629 (4)	8024 (6)	49 (2)
C(34)	1150 (11)	2487 (4)	8883 (7)	65 (3)
C(35)	385 (12)	1595 (5)	8594 (9)	84 (4)
C(36)	-162 (11)	3192 (6)	8506 (9)	83 (3)
C(37)	1946 (17)	2590 (7)	10441 (8)	111 (5)
B	3661 (8)	2813 (4)	4590 (7)	41 (2)

^a Equivalent isotropic U defined as one-third of the trace of the orthogonalized U_{ij} tensor.



$\text{HB(3-Bu}^i\text{pz)}_3\text{CoF}$, has also been characterized by X-ray diffraction techniques (Figure 3). Atomic coordinates and thermal parameters for non-hydrogen atoms are listed in Table VII, and selected bond distances and angles are listed in Tables VIII and IX.

The abstraction of the fluoride ligand in the above reactions of the chloride derivatives with AgBF_4 is presumably a result of the potent Lewis acidity of the 3-coordinate metal cation intermediates, $[\{\eta^3\text{-HB(3-Bu}^i\text{pz)}_3\}\text{M}]^+$. Although the formation of fluoride complexes as a result of decomposition of transition-metal tetrafluoroborate derivatives is well-known,⁸ the formation of the

**Figure 3.** ORTEP diagram of $\{\eta^3\text{-HB(3-Bu}^i\text{pz)}_3\}\text{CoF}$. For clarity, thermal ellipsoids are shown at 20% probability.**Table VIII.** Bond Lengths (\AA) for $\{\eta^3\text{-HB(3-Bu}^i\text{pz)}_3\}\text{CoF}$

Co-F	2.060 (3)	Co-N(12)	2.046 (5)
Co-N(22)	2.040 (5)	Co-N(32)	2.056 (4)
N(11)-N(12)	1.392 (7)	N(11)-C(11)	1.343 (8)
N(11)-B	1.542 (8)	N(12)-C(13)	1.343 (7)
N(21)-N(22)	1.374 (7)	N(21)-C(21)	1.357 (9)
N(21)-B	1.533 (8)	N(22)-C(23)	1.360 (8)
N(31)-N(32)	1.368 (7)	N(31)-C(31)	1.332 (8)
N(31)-B	1.553 (8)	N(32)-C(33)	1.340 (7)
C(11)-C(12)	1.384 (9)	C(12)-C(13)	1.402 (9)
C(13)-C(14)	1.509 (8)	C(14)-C(15)	1.536 (10)
C(14)-C(16)	1.544 (10)	C(14)-C(17)	1.530 (9)
C(21)-C(22)	1.370 (10)	C(22)-C(23)	1.397 (11)
C(23)-C(24)	1.537 (10)	C(24)-C(25)	1.504 (11)
C(24)-C(26)	1.478 (11)	C(24)-C(27)	1.564 (13)
C(31)-C(32)	1.369 (10)	C(32)-C(33)	1.380 (10)
Cf(33)-C(34)	1.523 (12)	C(34)-C(35)	1.523 (11)
C(34)-C(36)	1.545 (12)	C(34)-C(37)	1.552 (10)

Table IX. Bond Angles (deg) for $\{\eta^3\text{-HB(3-Bu}^i\text{pz)}_3\}\text{CoF}$

F-Co-N(12)	123.8 (2)	F-Co-N(22)	123.1 (2)
N(12)-Co-N(22)	93.6 (2)	F-Co-N(32)	118.5 (2)
N(12)-Co-N(32)	95.0 (2)	N(22)Co-N(32)	95.8 (2)
N(12)-N(11)-C(11)	108.2 (4)	N(12)-N(11)-B	122.2 (4)
C(11)-N(11)-B	129.5 (5)	Co-N(12)-N(11)	109.0 (3)
Co-N(12)-C(13)	142.9 (4)	N(11)-N(12)-C(13)	108.1 (4)
N(22)-N(21)-C(21)	108.7 (5)	N(22)-N(21)-B	122.7 (5)
C(21)-N(21)-B	128.6 (5)	Co-N(22)-N(21)	109.5 (3)
Co-N(22)-C(23)	143.2 (5)	N(21)-N(22)-C(23)	107.3 (5)
N(32)-N(31)-C(31)	109.3 (5)	N(32)-N(31)-B	121.2 (4)
C(31)-N(31)-B	129.5 (5)	Co-N(32)-N(31)	110.4 (3)
Co-N(32)-C(33)	142.4 (5)	N(31)-N(32)-C(33)	107.1 (5)
N(11)-C(11)-C(12)	109.0 (6)	C(11)-C(12)-C(13)	106.3 (5)
N(12)-C(13)-C(12)	108.5 (5)	N(12)-C(13)-C(14)	121.4 (5)
C(12)-C(13)-C(14)	130.0 (5)	C(13)-C(14)-C(15)	108.9 (5)
C(13)-C(14)-C(16)	109.5 (5)	C(15)-C(14)-C(16)	109.0 (6)
C(13)-C(14)-C(17)	110.8 (5)	C(15)-C(14)-C(17)	110.2 (5)
C(16)-C(14)-C(17)	108.4 (5)	N(21)-C(21)-C(22)	108.8 (6)
C(21)-C(22)-C(23)	106.4 (6)	N(22)-C(23)-C(22)	108.7 (6)
N(22)-C(23)-C(24)	120.0 (6)	C(22)-C(23)-C(24)	131.3 (6)
C(23)-C(24)-C(25)	109.6 (6)	C(23)-C(24)-C(26)	110.3 (6)
C(25)-C(24)-C(26)	112.9 (8)	C(23)-C(24)-C(27)	107.9 (7)
C(25)-C(24)-C(27)	107.2 (7)	C(26)-C(24)-C(27)	108.8 (7)
N(31)-C(31)-C(32)	108.3 (6)	C(31)-C(32)-C(33)	106.5 (6)
N(32)-C(33)-C(32)	108.9 (6)	N(32)-C(33)-C(34)	121.3 (6)
C(32)-C(33)-C(34)	129.7 (6)	C(33)-C(34)-C(35)	110.8 (6)
C(33)-C(34)-C(36)	109.3 (6)	C(35)-C(34)-C(36)	109.4 (7)
C(33)-C(34)-C(37)	106.9 (8)	C(35)-C(34)-C(37)	111.5 (7)
C(36)-C(34)-C(37)	109.9 (7)	N(11)-B-N(21)	109.7 (4)
N(11)-B-N(31)	109.3 (5)	N(21)-B-N(31)	108.0 (5)

fluoro complexes $\{\eta^3\text{-HB(3-Bu}^i\text{pz)}_3\}\text{MF}$ ($M = \text{Fe, Co}$) from $\{\eta^3\text{-HB(3-Bu}^i\text{pz)}_3\}\text{MCl}$ and AgBF_4 are particularly facile examples

- (8) (a) Reedijk, J. *Comments Inorg. Chem.* **1982**, *1*, 379-389. (b) Hitchcock, P. B.; Lappert, M. F.; Taylor, R. G. J. *Chem. Soc., Chem. Commun.* **1984**, 1082-1084. (c) Holt, E. M.; Hlatky, G. G.; Crabtree, R. H. *J. Am. Chem. Soc.* **1983**, *105*, 7302-7306. (d) Thomas, R. R.; Chebolu, V.; Sen, A. *J. Am. Chem. Soc.* **1986**, *108*, 4096-4103.

Table X. Crystallographic Data for $\{\eta^3\text{-HB(3-Bu}^i\text{pz)}_3\}\text{FeCl}$, $\{\eta^3\text{-HB(3-Bu}^i\text{pz)}_3\}\text{CoCl}$, and $\{\eta^3\text{-HB(3-Bu}^i\text{pz)}_3\}\text{CoF}$

	$\{\eta^3\text{-HB(3-Bu}^i\text{pz)}_3\}\text{FeCl}$	$\{\eta^3\text{-HB(3-Bu}^i\text{pz)}_3\}\text{CoCl}$	$\{\eta^3\text{-HB(3-Bu}^i\text{pz)}_3\}\text{CoF}$
formula	$\text{C}_{21}\text{H}_{34}\text{N}_6\text{BFeCl}$	$\text{C}_{21}\text{H}_{34}\text{N}_6\text{BCoCl}$	$\text{C}_{21}\text{H}_{34}\text{N}_6\text{BCoF}$
fw	472.7	475.7	448.5
lattice	orthorhombic	orthorhombic	monoclinic
cell constants, Å, deg, and Å ³	$a = 16.075$ (5) $b = 15.958$ (4) $c = 9.792$ (4) $V = 2512$ (1)	$a = 16.024$ (1) $b = 15.966$ (3) $c = 9.769$ (4) $V = 2499$ (1)	$a = 8.402$ (5) $b = 15.414$ (6) $c = 9.722$ (1) $\beta = 100.237$ (3) $V = 1239$ (1)
Z	4	4	2
space group	<i>Pnma</i> (No. 62)	<i>Pnma</i> (No. 62)	<i>P1n1</i> (No. 7)
T	room temp	room temp	room temp
radiation (λ , Å)	Mo K α (0.71073)	Mo K α (0.71073)	Mo K α (0.71073)
ρ (calcd), g cm ⁻³	1.25	1.26	1.23
μ (calcd), cm ⁻¹	7.4	8.4	7.5
R	4.44	4.54	4.79
R_w^a	4.61	4.85	5.74

^a Weighting scheme $w = [\sigma^2(F) + gF^2]^{-1}$.

of fluoride ligand abstraction and thus further question the role of $[\text{BF}_4]^-$ as a noncoordinating ion.⁹

Experimental Details

General Considerations. All manipulations were performed by using a combination of glovebox, high-vacuum, or Schlenk techniques.¹⁰ Solvents were purified and degassed by standard procedures. ¹H NMR spectra were measured on a Varian VXR 200 spectrometer. IR spectra were recorded as Nujol mulls on a Perkin-Elmer 1420 spectrophotometer. Mass spectra were obtained on a Nermag R10-10 mass spectrometer by using chemical ionization (NH_3) techniques. Elemental analyses were determined with a Perkin-Elmer 2400 CHN elemental analyzer. $\text{Ti}\{\text{HB(3-Bu}^i\text{pz)}_3\}$ was prepared by the literature method.³

Synthesis of $\{\eta^3\text{-HB(3-Bu}^i\text{pz)}_3\}\text{FeCl}$. A solution of $\text{Ti}\{\text{HB(3-Bu}^i\text{pz)}_3\}$ (1.0 g, 1.7 mmol) in acetone (20 mL) was added to a stirred suspension of FeCl_2 (210 mg, 1.7 mmol) in acetone (10 mL). A white precipitate (TiCl) formed immediately. The mixture was filtered, and the filtrate was concentrated and cooled to 0 °C, depositing $\{\eta^3\text{-HB(3-Bu}^i\text{pz)}_3\}\text{FeCl}$ as white crystals. $\{\eta^3\text{-HB(3-Bu}^i\text{pz)}_3\}\text{FeCl}$ was isolated by filtration and dried in vacuo. Yield of $\{\eta^3\text{-HB(3-Bu}^i\text{pz)}_3\}\text{FeCl}$: 220 mg (28%). Anal. Calcd: C, 53.4; H, 7.3; N, 17.8. Found: C, 53.1; H, 7.74; N, 17.7. IR data (Nujol mull, KBr plates, cm^{-1}): 2523 ($\nu_{\text{B-H}}$). MS: m/e 473 ($\text{M}^+ + \text{H}$). $\mu_{\text{eff}} = 5.7 \mu_{\text{B}}$ (room temperature, solid state). ¹H NMR (CDCl_3): δ -12.0, $[\eta^3\text{-HB}\{\text{C}_3\text{N}_2\text{H}_2\text{C}(\text{CH}_3)_3\}_3]$, 45.7 and 62.9 [$\eta^3\text{-HB}\{\text{C}_3\text{N}_2\text{H}_2\text{C}(\text{CH}_3)_3\}_3]$.

Synthesis of $\{\eta^3\text{-HB(3-Bu}^i\text{pz)}_3\}\text{MnCl}$. A solution of $\text{Ti}\{\text{HB(3-Bu}^i\text{pz)}_3\}$ (2.0 g, 3.4 mmol) in acetone (30 mL) was added to a stirred suspension of MnCl_2 (430 mg, 3.4 mmol) in acetone (20 mL). A white precipitate (TiCl) formed immediately. The mixture was filtered, and the filtrate was concentrated and cooled to 0 °C, depositing $\{\eta^3\text{-HB(3-Bu}^i\text{pz)}_3\}\text{MnCl}$ as white crystals. $\{\eta^3\text{-HB(3-Bu}^i\text{pz)}_3\}\text{MnCl}$ was isolated by filtration and dried in vacuo. Yield of $\{\eta^3\text{-HB(3-Bu}^i\text{pz)}_3\}\text{MnCl}$: 910 mg (57%). Anal. Calcd: C, 53.5; H, 7.3; N, 17.8. Found: C, 53.6; H, 7.5; N, 17.0. IR data (Nujol mull, KBr plates, cm^{-1}): 2519 ($\nu_{\text{B-H}}$). MS: m/e 472 ($\text{M}^+ + \text{H}$).

Synthesis of $\{\eta^3\text{-HB(3-Bu}^i\text{pz)}_3\}\text{CoCl}$. A solution of $\text{Ti}\{\text{HB(3-Bu}^i\text{pz)}_3\}$ (500 mg, 0.85 mmol) in acetone (10 mL) was added to a solution of CoCl_2 (110 mg, 0.85 mmol) in acetone (10 mL). A white precipitate (TiCl) formed immediately. The mixture was filtered, and the filtrate was concentrated and cooled to 0 °C, depositing $\{\eta^3\text{-HB(3-Bu}^i\text{pz)}_3\}\text{CoCl}$ as blue crystals. $\{\eta^3\text{-HB(3-Bu}^i\text{pz)}_3\}\text{CoCl}$ was isolated by filtration and dried in vacuo. Yield of $\{\eta^3\text{-HB(3-Bu}^i\text{pz)}_3\}\text{CoCl}$: 160 mg (40%). MS: m/e 476 ($\text{M}^+ + \text{H}$). ¹H NMR (CDCl_3): δ 8.5 [$\eta^3\text{-HB}\{\text{C}_3\text{N}_2\text{H}_2\text{C}(\text{CH}_3)_3\}_3]$, 31.6 and 74.3 [$\eta^3\text{-HB}\{\text{C}_3\text{N}_2\text{H}_2\text{C}(\text{CH}_3)_3\}_3]$.

Synthesis of $\{\eta^3\text{-HB(3-Bu}^i\text{pz)}_3\}\text{NiCl}$. A solution of $\text{Ti}\{\text{HB(3-Bu}^i\text{pz)}_3\}$ (500 mg, 0.85 mmol) in acetone (10 mL) was added to a solution of $\text{NiCl}_2 \cdot 6\text{H}_2\text{O}$ (200 mg, 0.84 mmol) in ethanol (10 mL). A white precipitate (TiCl) formed immediately. The mixture was filtered, and the filtrate was concentrated and cooled to 0 °C, depositing $\{\eta^3\text{-HB(3-Bu}^i\text{pz)}_3\}\text{NiCl}$ as purple crystals. $\{\eta^3\text{-HB(3-Bu}^i\text{pz)}_3\}\text{NiCl}$ was isolated by filtration and dried in vacuo. Yield of $\{\eta^3\text{-HB(3-Bu}^i\text{pz)}_3\}\text{NiCl}$: 160 mg (40%). MS: m/e 475 ($\text{M}^+ + \text{H}$). ¹H NMR (CDCl_3): δ 2.2 [$\eta^3\text{-HB}\{\text{C}_3\text{N}_2\text{H}_2\text{C}(\text{CH}_3)_3\}_3]$, 19.4 and 81.0 [$\eta^3\text{-HB}\{\text{C}_3\text{N}_2\text{H}_2\text{C}(\text{CH}_3)_3\}_3]$.

Synthesis of $\{\eta^3\text{-HB(3-Bu}^i\text{pz)}_3\}\text{FeF}$. A solution of AgBF_4 (80 mg, 0.4 mmol) in CH_2Cl_2 was added to a stirred solution of $\{\eta^3\text{-HB(3-Bu}^i\text{pz)}_3\}\text{FeCl}$ (180 mg, 0.4 mmol) in CH_2Cl_2 at room temperature. A white precipitate (AgCl) formed immediately. The mixture was filtered, the solvent was removed from the filtrate under reduced pressure at room temperature, the residue obtained was extracted into benzene (5 mL), and the solvent was removed under reduced pressure at room temperature. The product was recrystallized from CH_2Cl_2 and dried in vacuo, giving $\{\eta^3\text{-HB(3-Bu}^i\text{pz)}_3\}\text{FeF}$ as a white solid (30 mg, 17%). Anal. Calcd: C, 55.3; H, 7.5; N, 18.4. Found: C, 55.3; H, 7.8; N, 15.6. IR data (Nujol mull, KBr plates, cm^{-1}): 2529 ($\nu_{\text{B-H}}$). MS: m/e 457 ($\text{M}^+ + \text{H}$). ¹H NMR (CDCl_3): δ -21.7 [$\eta^3\text{-HB}\{\text{C}_3\text{N}_2\text{H}_2\text{C}(\text{CH}_3)_3\}_3]$, 59.2 and 63.8 [$\eta^3\text{-HB}\{\text{C}_3\text{N}_2\text{H}_2\text{C}(\text{CH}_3)_3\}_3]$.

Synthesis of $\{\eta^3\text{-HB(3-Bu}^i\text{pz)}_3\}\text{CoF}$. A solution of AgBF_4 (65 mg, 0.33 mmol) in CH_2Cl_2 was added to a stirred solution of $\{\eta^3\text{-HB(3-Bu}^i\text{pz)}_3\}\text{CoCl}$ (160 mg, 0.33 mmol) in CH_2Cl_2 at room temperature. A white precipitate (AgCl) formed immediately. The mixture was filtered, the solvent was removed from the filtrate under reduced pressure at room temperature, and the residue was extracted with benzene (5 mL). The solvent was removed under reduced pressure, and the solid was recrystallized from Et_2O , giving $\{\eta^3\text{-HB(3-Bu}^i\text{pz)}_3\}\text{CoF}$ as a blue-purple solid (46 mg, 31%). Anal. Calcd: C, 54.9; H, 7.5; N, 18.3. Found: C, 54.0; H, 7.5; N, 16.6. IR data (Nujol mull, KBr plates, cm^{-1}): 2545 ($\nu_{\text{B-H}}$). MS: m/e 460 ($\text{M}^+ + \text{H}$). ¹H NMR (CDCl_3): δ 2.9 [$\eta^3\text{-HB}\{\text{C}_3\text{N}_2\text{H}_2\text{C}(\text{CH}_3)_3\}_3]$, 44.5 and 71.6 [$\eta^3\text{-HB}\{\text{C}_3\text{N}_2\text{H}_2\text{C}(\text{CH}_3)_3\}_3]$.

X-ray Structure Determination of $\{\eta^3\text{-HB(3-Bu}^i\text{pz)}_3\}\text{FeCl}$. Crystal data, data collection, and refinement parameters are summarized in Table X. A single colorless crystal of $\{\eta^3\text{-HB(3-Bu}^i\text{pz)}_3\}\text{FeCl}$, grown from CH_2Cl_2 at room temperature, was mounted in a glass capillary and placed on a Nicolet R3M diffractometer using graphite-monochromated Mo K α X-radiation ($\lambda = 0.71073$ Å). The unit was determined by the automatic indexing of 25 centered reflections and confirmed by examination of the axial photographs. Three check reflections were measured every 100 reflections, and the Wyckoff data set was scaled accordingly and corrected for Lorentz, polarization, and absorption effects. The intensity of 2986 unique reflections in the range $3 \leq 2\theta \leq 55^\circ$ (h, k, l) were measured, of which 1045 with $F > 6\sigma(F)$ were used in the structure determination. The structure was solved by using direct methods and standard difference map techniques on a Data General NOVA 4 computer using SHELXTL.¹¹ Systematic absences were consistent with either the *Pnma* or *Pna2*₁ space group, but *E*-value statistics strongly favored the centrosymmetric alternative, *Pnma*. Most of the hydrogen atoms were located in the difference map after all the non-hydrogen atoms were located and refined anisotropically, but hydrogens on carbon were allowed to refine in calculated positions ($d_{\text{C-H}} = 0.96$ Å; $U_{\text{iso}}(\text{H}) = 1.2U_{\text{iso}}(\text{C})$). Block-diagonal least-squares refinement converged to $R = 4.44$ ($R_w = 4.61$) with a goodness-of-fit = 1.15 for 155 parameters. The final difference map showed no significant features, with the highest final peak 0.31 e Å⁻³ near Fe. Atomic coordinates and thermal parameters for non-hydrogen atoms are listed in Table I, and selected bond distances and angles are listed in Tables II and III.

X-ray Structure Determination of $\{\eta^3\text{-HB(3-Bu}^i\text{pz)}_3\}\text{CoCl}$. Crystal data, data collection, and refinement parameters are summarized in Table X. Intensity data collection and processing procedures are as

(9) Honeychuck, R. V.; Hersh, W. H. *Inorg. Chem.* **1989**, *28*, 2869-2886 and references therein.

(10) (a) McNally, J. P.; Leong, V. S.; Cooper, N. J. *ACS Symp. Ser.* **1987**, No. 357, 6-23. (b) Burger, B. J.; Bercaw, J. E. *ACS Symp. Ser.* **1987**, No. 357, 79-97.

(11) Sheldrick, G. M. SHELXTL, An Integrated System for Solving, Refining and Displaying Crystal Structures from Diffraction Data. University of Göttingen, Göttingen, Federal Republic of Germany, 1981.

described for $\{\eta^3\text{-HB(3-Bu}^i\text{pz)}_3\}_3\text{FeCl}$. The intensity of 3451 unique reflections in the range $3 \leq 2\theta \leq 58^\circ$ (h, k, l) were measured, of which 1249 with $F > 6\sigma(F)$ were used in the structure determination. Systematic absences were consistent with either $Pnma$ or $Pna2_1$ space groups, but E -value statistics strongly favored the centrosymmetric alternative, $Pnma$. Most of the hydrogen atoms were located in the difference map after all the non-hydrogen atoms were located and refined anisotropically, but hydrogens on carbon were allowed to refine in calculated positions ($d_{\text{C-H}} = 0.96 \text{ \AA}$; $U_{\text{iso}}(\text{H}) = 1.2U_{\text{iso}}(\text{C})$). Block-diagonal least-squares refinement converged to $R = 4.54$ ($R_w = 4.85$) with a goodness-of-fit = 1.21 for 155 parameters. The final difference map showed no significant features, with the highest final peak 0.37 e \AA^{-3} . Atomic coordinates and thermal parameters for non-hydrogen atoms are listed in Table IV, and selected bond distances and angles are listed in Tables V and VI.

X-ray Structure Determinations of $\{\eta^3\text{-HB(3-Bu}^i\text{pz)}_3\}_3\text{CoF}$. Crystal data, data collection, and refinement parameters are summarized in Table X. Intensity data collection and processing procedures are as described for $\{\eta^3\text{-HB(3-Bu}^i\text{pz)}_3\}_3\text{FeCl}$, with the exception that an absorption correction was not applied. The intensity of 3833 unique reflections in the range $3 \leq 2\theta \leq 60^\circ$ ($h, k, \pm l$) were measured, of which

2319 with $F > 6\sigma(F)$ were used in the structure determination. Systematic absences were consistent with either the $P1n1$ or $P12/n1$ space group, but E -value statistics strongly favored the noncentrosymmetric alternative, $P1n1$. Most of the hydrogen atoms were located in the difference map after all the non-hydrogen atoms were located and refined anisotropically, but hydrogens on carbon were allowed to refine in calculated positions ($d_{\text{C-H}} = 0.96 \text{ \AA}$; $U_{\text{iso}}(\text{H}) = 1.2U_{\text{iso}}(\text{C})$). Block-diagonal least-squares refinement converged to $R = 4.79$ ($R_w = 5.74$) with a goodness-of-fit = 1.29 for 273 parameters. The final difference map showed no significant features, with the highest final peak 0.62 e \AA^{-3} . Atomic coordinates and thermal parameters for non-hydrogen atoms are listed in Table VII, and selected bond distances and angles are listed in Tables VIII and IX.

Supplementary Material Available: Tables SI–SIX, listing crystal and intensity collection data, hydrogen atomic coordinates, and anisotropic displacement parameters for $\{\eta^3\text{-HB(3-Bu}^i\text{pz)}_3\}_3\text{FeCl}$, $\{\eta^3\text{-HB(3-Bu}^i\text{pz)}_3\}_3\text{CoCl}$, and $\{\eta^3\text{-HB(3-Bu}^i\text{pz)}_3\}_3\text{CoF}$ (9 pages); tables of calculated and observed structure factors (28 pages). Ordering information is given on any current masthead page.

Contribution from the Department of Chemistry,
Frick Laboratory, Princeton University, Princeton, New Jersey 08544-1009

Multielectron Transfer and Single-Crystal X-ray Structure of a Trinuclear Cyanide-Bridged Platinum–Iron Species

Meisheng Zhou, Brian W. Pfennig, Jana Steiger, Donna Van Engen, and Andrew B. Bocarsly*

Received October 19, 1989

$[\text{Pt}(\text{NH}_3)_4]_2[(\text{NC})_5\text{Fe}^{\text{II}}\text{-CN-Pt}^{\text{IV}}(\text{NH}_3)_4\text{-NC-Fe}^{\text{II}}(\text{CN})_5] \cdot 9\text{H}_2\text{O}$ was synthesized by the redox reaction of $\text{Pt}(\text{NH}_3)_4(\text{NO}_3)_2$ and $\text{K}_3\text{Fe}(\text{CN})_6$ in aqueous solution. The red complex crystallized in space group $P2_1/c$ (No. 14) and was analyzed by X-ray diffractometry. The monoclinic crystal consists of a trinuclear, cyanide-bridged Fe–Pt–Fe anion hydrogen-bonded via a terminal cyanide group on each iron atom to two separate tetraammineplatinum(II) counterions. Unit cell dimensions are $a = 15.313$ (2) \AA , $b = 8.5353$ (14) \AA , $c = 16.206$ (5) \AA , $\beta = 100.52$ (2) $^\circ$, and $Z = 2$; a center of inversion exists at the central Pt atom of the trinuclear anion. The R factors for this structure are $R = 5.0\%$ and $R_w = 5.3\%$. On the basis of infrared spectroscopy, magnetic measurements, ESR spectroscopy, and the electrochemistry of the compound, localized oxidation states of $\text{Fe}^{\text{II}}\text{-Pt}^{\text{IV}}\text{-Fe}^{\text{II}}$ are assigned to the complex. The electronic spectrum reveals an intervalent (IT) charge-transfer absorption at approximately 470 nm. Excitation into this band effects an electron transfer between the Fe^{II} and Pt^{IV} atoms and results in the formation of $\text{Pt}(\text{NH}_3)_4^{2+}$ and ferricyanide in a 1 to 2 ratio. The initial quantum yield for the formation of ferricyanide at 488-nm irradiation is 0.02.

Introduction

Inorganic donor/acceptor complexes containing intervalent (IT) or metal to metal charge-transfer (MMCT) bands have received significant attention in the last decade due to their potential applications to solar energy conversion and/or photocatalysis. Homobinuclear mixed-valent transition-metal complexes, particularly those of ruthenium, have been extensively investigated.¹ These compounds exhibit IT absorptions at low energies, whereas these transitions often occur in the visible region of the spectrum in the heterobinuclear complexes due to the redox asymmetry of the metal centers.² Inorganic donor/acceptor complexes can be classified into two general types: contact ion pairs and linkage isomers. Binuclear examples of both types have been well characterized. Cyanide is often employed as a bridging ligand since MLCT bands with this ligand occur at high energies and do not obscure the observation of IT transitions in the visible electronic spectrum.³ Many of the cyanide-bridged species have been demonstrated to undergo inner sphere electron transfer upon irradiation into their respective IT absorption bands.⁴ However, only a handful of intervalent transition-metal complexes containing three (or more) metal centers have been characterized,^{5,6} and none of these, to the best of our knowledge, demonstrate photochemistry involving all three metals. Furthermore, the detailed structures of these multinuclear species have never been determined. We herein report the synthesis, characterization, chemistry, and crystal structure of the trinuclear, cyanide-bridged complex $\{[\text{Pt}(\text{NH}_3)_4]_2^{4+}\}[\{(\text{NC})_5\text{Fe}^{\text{II}}\text{-CN-Pt}^{\text{IV}}(\text{NH}_3)_4\text{-NC-Fe}^{\text{II}}(\text{CN})_5\}^{4-}] \cdot 9\text{H}_2\text{O}$.

Not only does this complex exhibit an IT absorption in the visible region of the optical spectrum, but we find that irradiation into this absorption leads to a two-electron charge transfer involving all three metal centers.

Vogler et al. have recently reported the synthesis of the trinuclear compound $[(\text{bpy})(\text{H}_2\text{O})\text{Pt}^{\text{II}}\text{-NC-M}^{\text{II}}(\text{CN})_4\text{-CN-Pt}^{\text{II}}(\text{bpy})(\text{H}_2\text{O})]$ (where $\text{M} = \text{Fe, Ru, or Os}$ and $\text{bpy} = 2,2'$ -bipyridine),⁵ which holds a superficial similarity to the complex reported. Unlike the complex under consideration, this compound contains all three metals in their lowest formal oxidation states and was characterized solely by MLCT ($\text{M}^{\text{II}} \rightarrow \pi^*\text{-bpy}$) absorptions. Consistent with this spectral assignment, the complex

- (1) (a) Taube, H. *Ann. N.Y. Acad. Sci.* **1978**, *313*, 483. (b) Meyer, T. J. *Ann. N.Y. Acad. Sci.* **1978**, *313*, 496. (c) Meyer, T. J. *Acc. Chem. Res.* **1978**, *11*, 94. (d) Meyer, T. J. In *Mixed-Valence Compounds*; Brown, D. B., Ed.; NATO Advanced Study Institute Series, No. 58; Reidel: Dordrecht, The Netherlands, 1980. (e) Creutz, C. *Prog. Inorg. Chem.* **1983**, *30*, 1.
- (2) Vogler, A.; Osman, A. H.; Kunkely, H. *Coord. Chem. Rev.* **1985**, *64*, 159.
- (3) Lever, A. B. P. *Inorganic Electronic Spectroscopy*; Elsevier: Amsterdam, 1985.
- (4) (a) Vogler, A.; Kunkely, H. *Ber. Bunsen-Ges. Phys. Chem.* **1975**, *79*, 83. (b) Vogler, A.; Kunkely, H. *Ber. Bunsen-Ges. Phys. Chem.* **1975**, *79*, 301. (c) Vogler, A.; Osman, A. H.; Kunkely, H. *Inorg. Chem.* **1987**, *26*, 2337. (d) Vogler, A.; Kisslinger, J. *J. Am. Chem. Soc.* **1982**, *104*, 2311.
- (5) Vogler, A.; Kunkely, H. *Inorg. Chim. Acta* **1988**, *150*, 1.
- (6) Bigozzi, C. A.; Roffia, S.; Scandola, F. *J. Am. Chem. Soc.* **1985**, *107*, 1644.

* To whom correspondence should be addressed.